

SUPPLEMENTARY INFORMATION FOR

Structural principles of nucleoside selectivity in a 2'-deoxyguanosine riboswitch

Olga Pikovskaya, Anna Polonskaia, Dinshaw J. Patel* and Alexander Serganov*[#],

Structural Biology Program, Memorial Sloan-Kettering Cancer Center, New York, New York,
USA

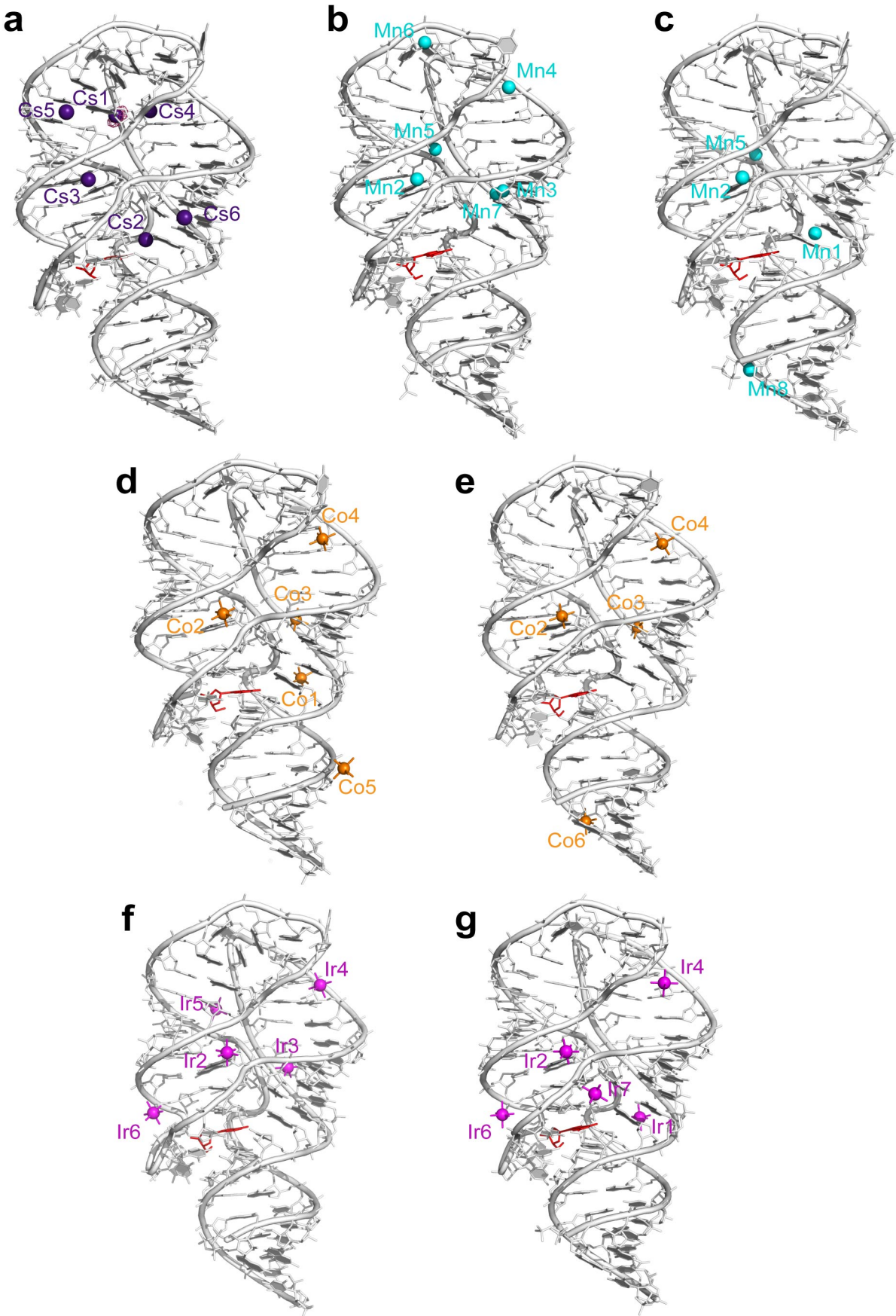
[#] Current affiliation: Department of Biochemistry, New York University School of Medicine,
New York, New York, USA

* e-mail: alexander.serganov@nyumc.org or pateld@mskcc.org

This PDF file includes:

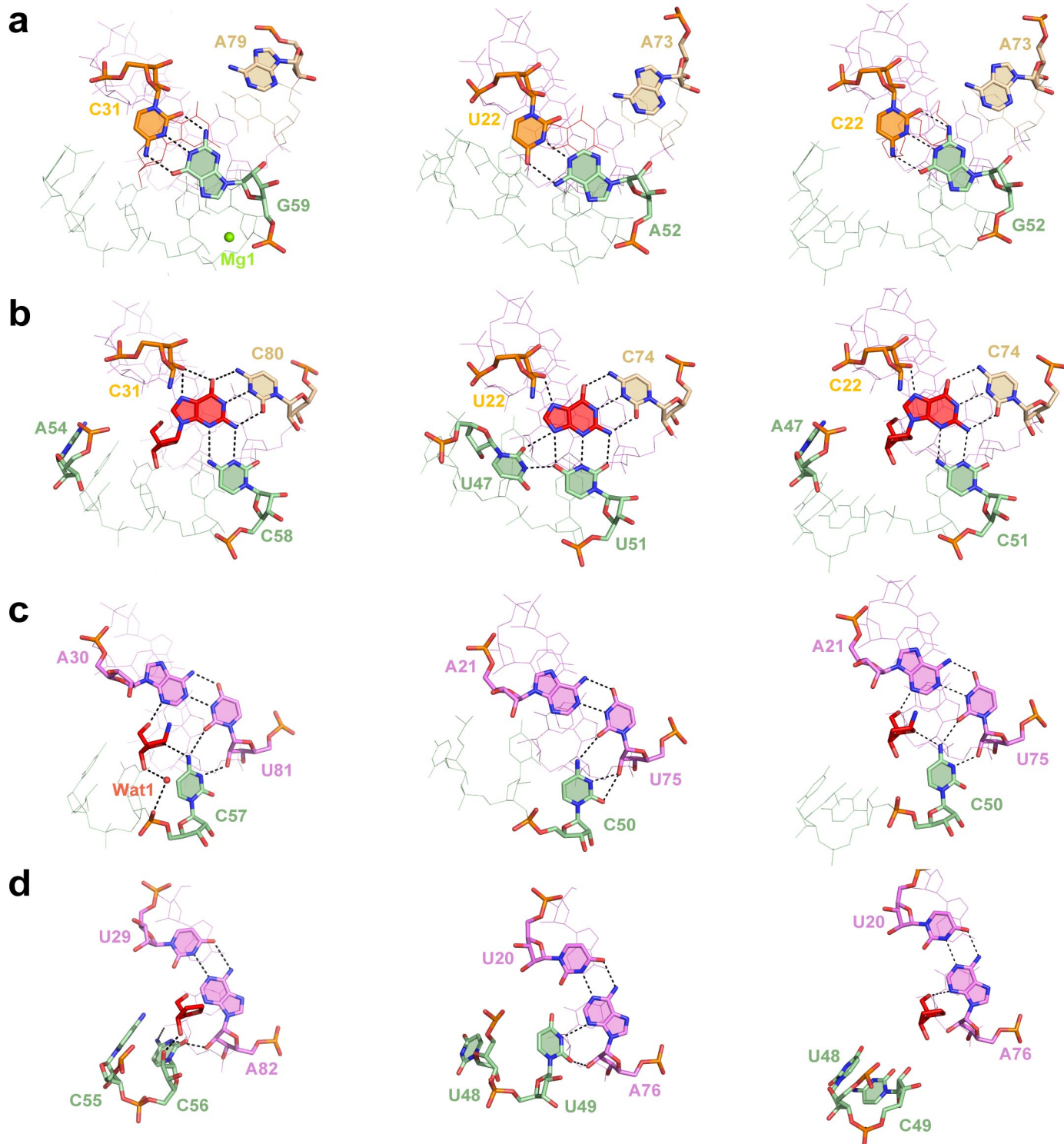
Supplementary Results

(Supplementary Figures 1-9 and Supplementary Tables 1-2)

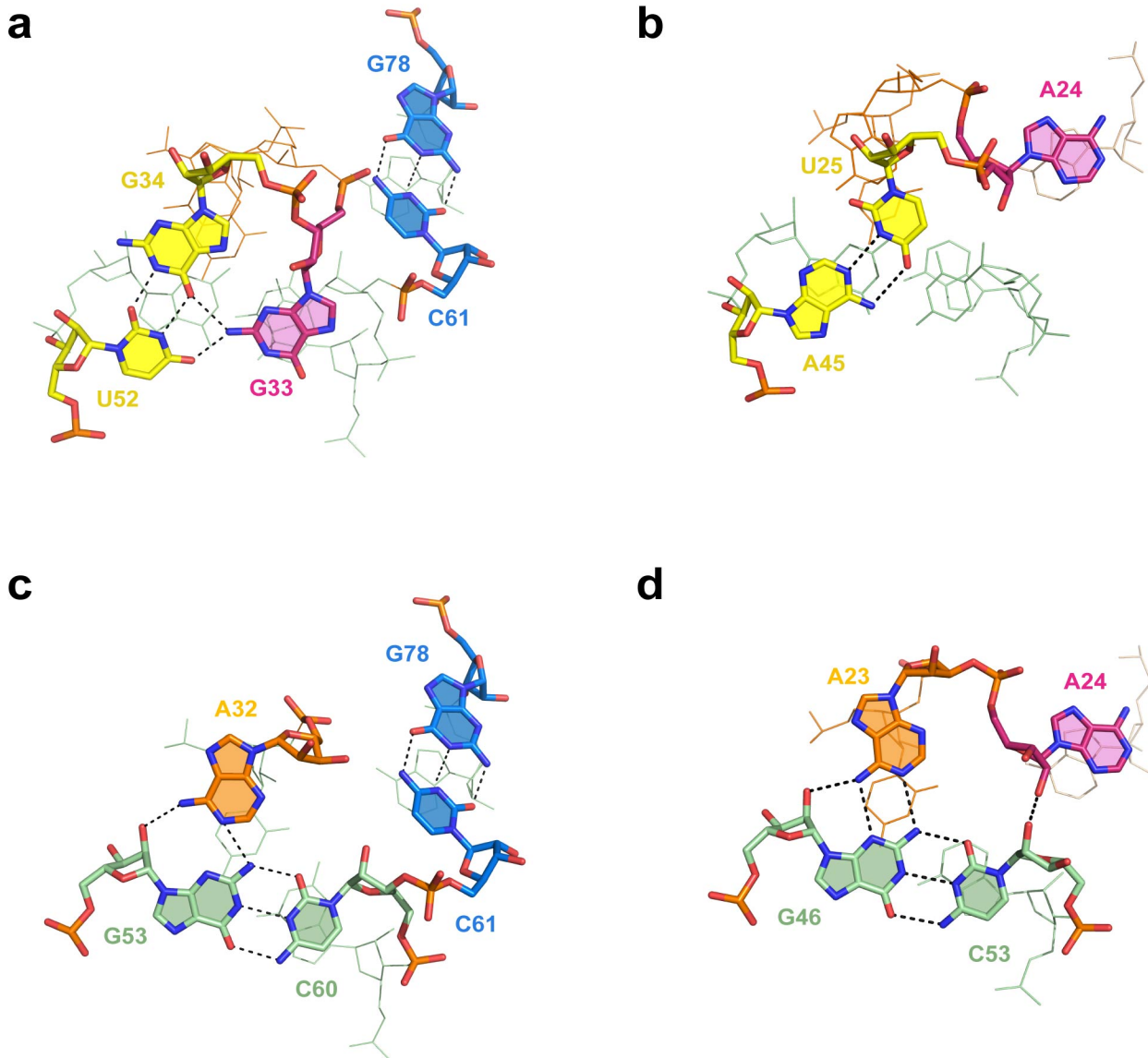


Supplementary Figure 2

Supplementary Figure 2. Metal cations in the dG-bound dG riboswitch structure observed using anomalous scattering after soaking crystals grown at low salt conditions in the metal salts. **a**, Cs⁺ cations (purple spheres). The refined riboswitch model (molecule A, PDB ID 3SKW) is shown with the anomalous difference electron density map (pink) contoured at 7 σ level. Anomalous and $2F_o - F_c$ maps for the cations around molecule B were much weaker and therefore Cs⁺ cations were not mapped in molecule B. **b** and **c**, Mn²⁺ cations (cyan) shown around the refined riboswitch models (PDB ID 3SKT) of molecules A and B, respectively. **d** and **e**, [Co(NH₃)₆]³⁺ cations (orange) shown together with the refined riboswitch models (PDB ID 3SKR) of molecules A and B, respectively. **f** and **g**, [Ir(NH₃)₆]³⁺ cations (magenta) shown together with the refined riboswitch models (PDB ID 3SKL) of molecules A and B, respectively.



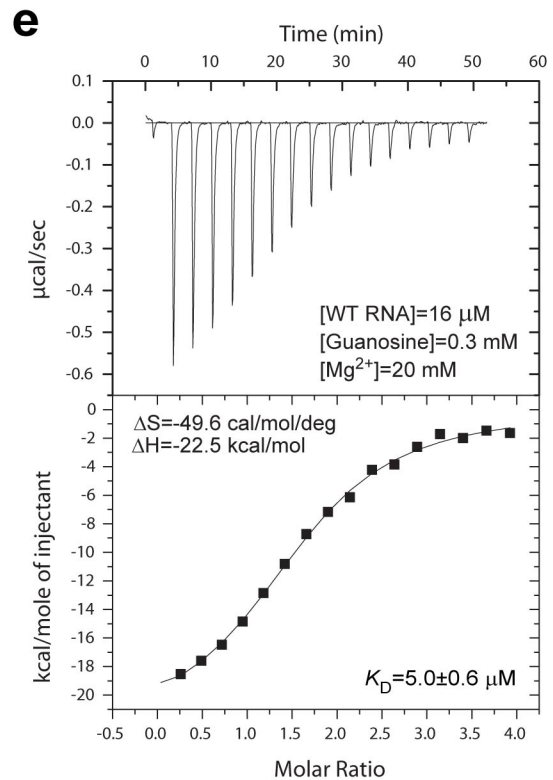
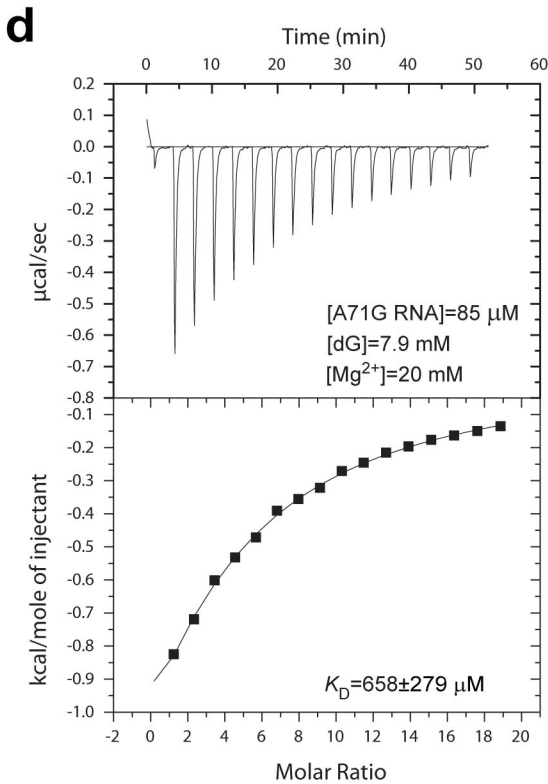
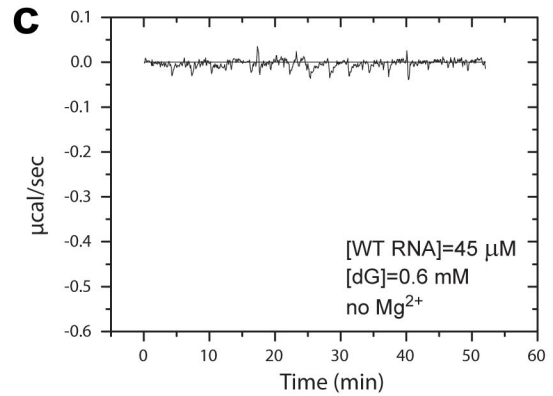
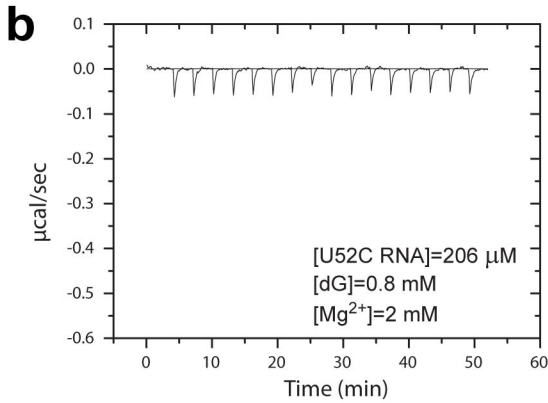
Supplementary Figure 3. Structural details of the guanine and dG binding pockets. Each lane corresponds to a section of the binding pocket from top to bottom. In all lanes, the left, middle and right panels show structures of the dG riboswitch bound to dG (current study, PDB code 3SKI), the guanine riboswitch bound to guanine¹⁵ (PDB code 1Y27), and the guanine-dG hybrid bound to dG¹⁷ (PDB code 3DSM), respectively. Dashed lines depict putative hydrogen bonds. **a**, A79 is positioned further from the C31-G59 base pair in the dG riboswitch than A73 is in the other two riboswitches. **b**, To accommodate the dG sugar, C58 in the dG riboswitch and C51 in the guanine-dG hybrid are shifted along dG. A54 (A47 in the hybrid) is rotated away from the binding pocket. **c**, The deoxyribose in the dG riboswitch and the guanine-dG hybrid is specifically recognized by nucleotides of the triple. **d**, To accommodate the sugar moiety, C56 is rotated as compared to U49 in the G riboswitch. In the guanine-dG hybrid, C49 is positioned away from A76 and does not participate in interactions with A76 and the dG sugar.



Supplementary Figure 4. Formation of base triples in the region above the ligand binding pocket in the dG and G riboswitches. Each section is shown from the top. In both lanes, the left panel shows the structure of the dG riboswitch bound to dG (current study, PDB code 3SKI) and the right panel shows the guanidine riboswitch bound to guanine¹⁵ (PDB code 1Y27). Dashed lines depict putative hydrogen bonds. **a**, G33 (in pink) participates in the formation of the G33•G34 platform and G33•(G34•U52) triple. **b**, In the G riboswitch, A24, analogous to C61 of the dG riboswitch, is positioned within the P3 hairpin and the triple is not formed. **c**, In the dG riboswitch, the C61-G78 base pair occupies the position of A24. The (C60-G53)•A32 triple is formed below the G33•(G34•U52) triple. **d**, In the G riboswitch, the (C53-G46)•A23 triple, reminiscent of the (C60-G53)•A32 triple, is formed below the U25-A45 base pair.

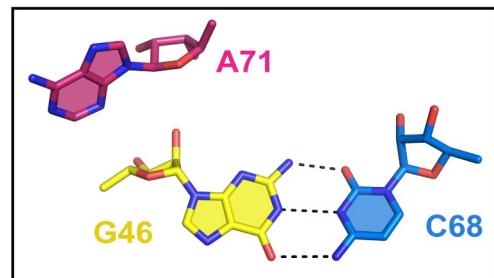
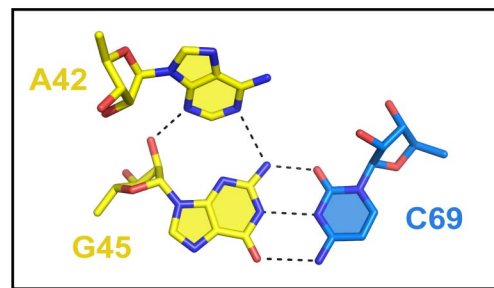
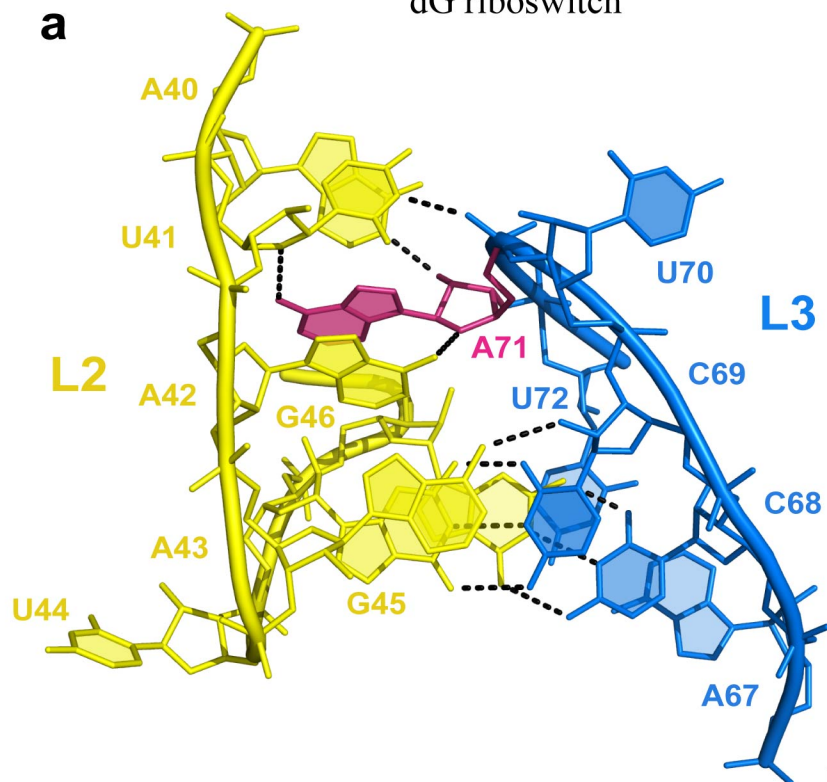
a

	2 mM [Mg ²⁺]			20 mM [Mg ²⁺]		
RNA	$K_D \pm \text{sd}$ (μM)	K_{rel}	N	$K_D \pm \text{sd}$ (μM)	K_{rel}	N
WT	0.30 \pm 0.15	-	1.08	0.10 \pm 0.01	-	1.16
G33U	2.57 \pm 0.23	8.6	1.00	0.21 \pm 0.05	2.1	1.04
G33A	15.10 \pm 0.20	50.3	1.13	0.62 \pm 0.17	6.2	1.13
U52C	ND	-	-	1.70 \pm 0.30	17.0	0.25

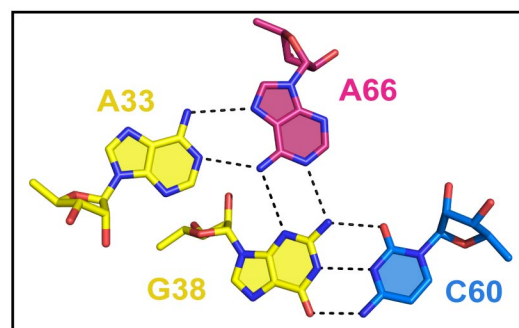
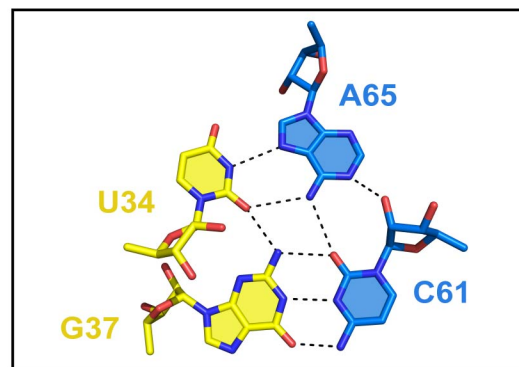
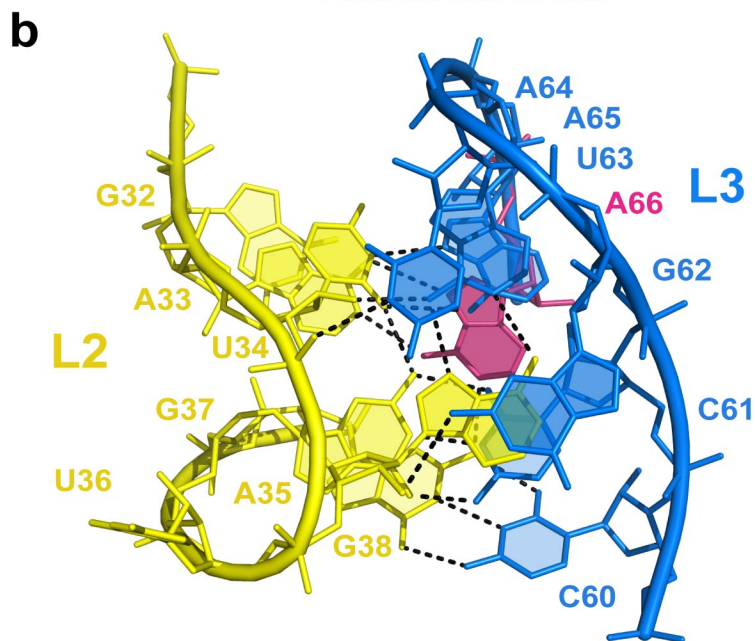


Supplementary Figure 5. Binding of ligands to the dG riboswitch measured by ITC. Raw measured heat changes as a function of time are supplemented with integrated heats of each injection in panels (d) and (e) (bottom part). **a**, Summary of binding affinities (mean $K_D \pm$ standard deviation) and the number of binding sites (mean N) for interactions between dG and wild type (WT) or mutant dG riboswitches determined by ITC in 20 mM and 2 mM Mg²⁺-containing solutions. K_{rel} is the ratio of K_D s for mutant and wild-type RNAs. ND, binding was not detected. **b**, Binding of dG to the U52C RNA was not detected in 2 mM Mg²⁺ conditions. **c**, Binding of dG to the wild type riboswitch was not detected in the absence of Mg²⁺ and in the presence of 0.5 mM EDTA. **d**, A71G RNA binds dG weakly. Since the binding affinity is outside of the optimal range for ITC measurements, the K_D value could not be determined with high accuracy. **e**, At 20 mM Mg²⁺, guanosine binds to the wild type dG riboswitch with a 50-fold reduced affinity in comparison to the dG binding affinity.

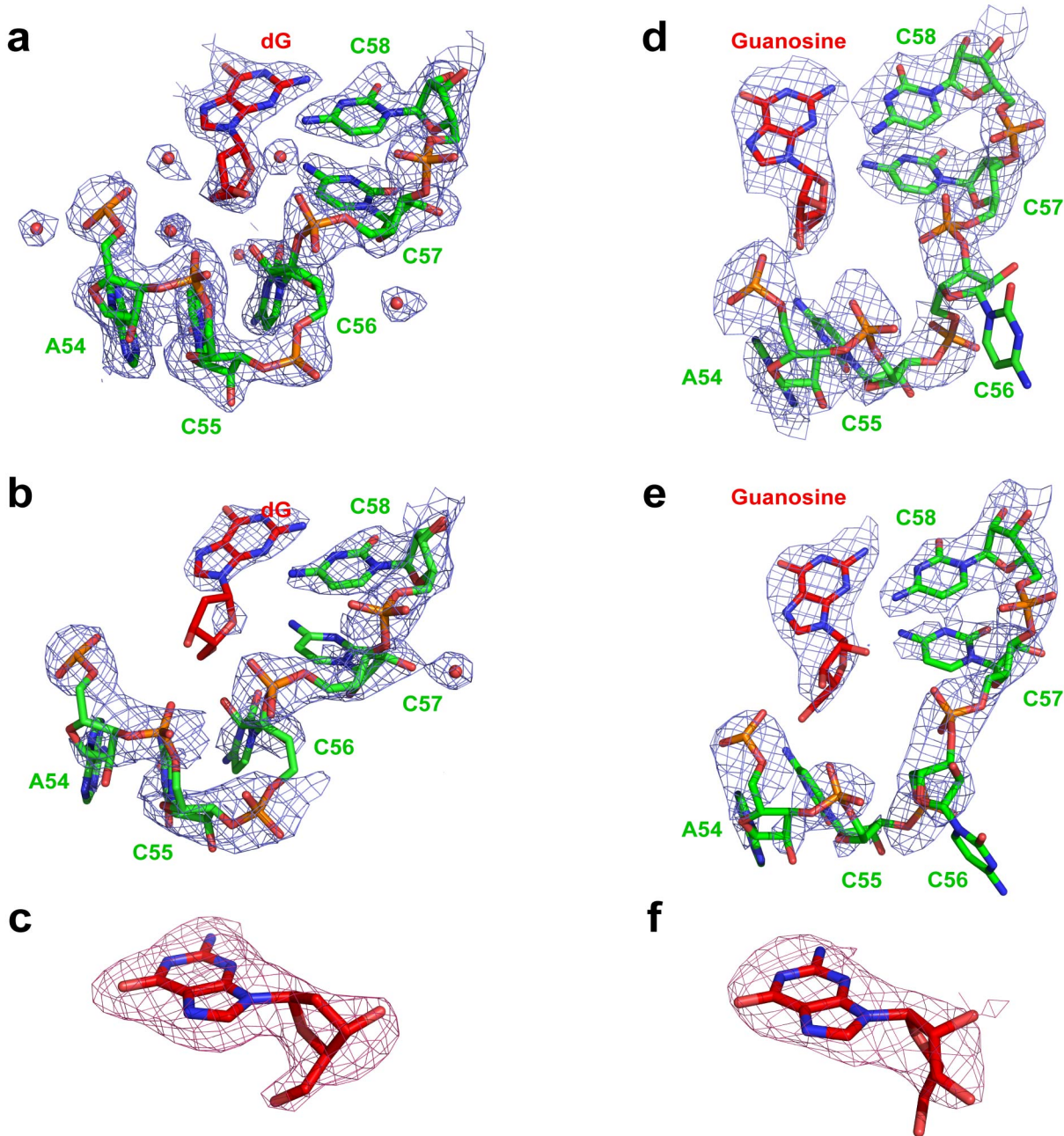
dG riboswitch



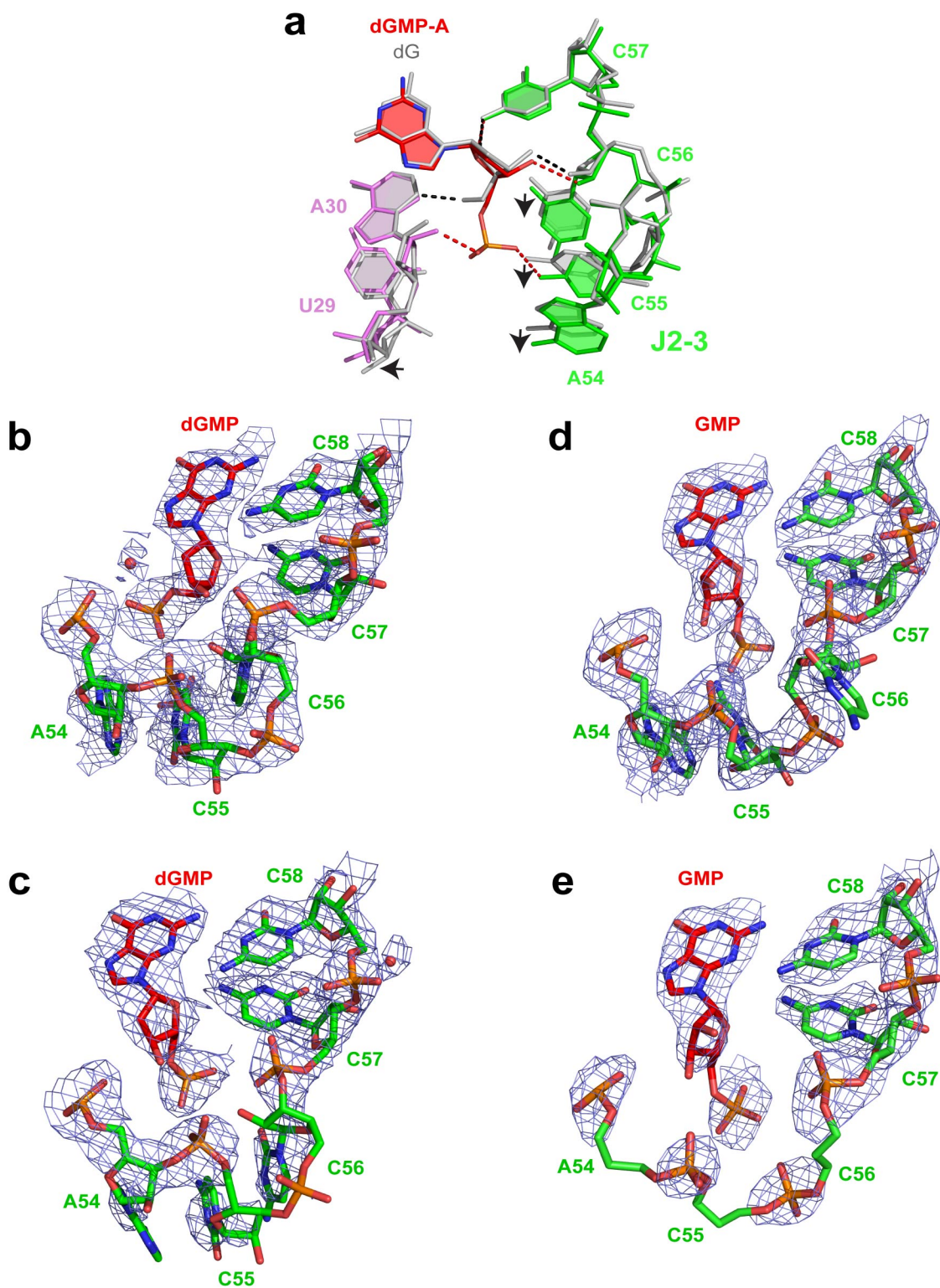
Guanine riboswitch



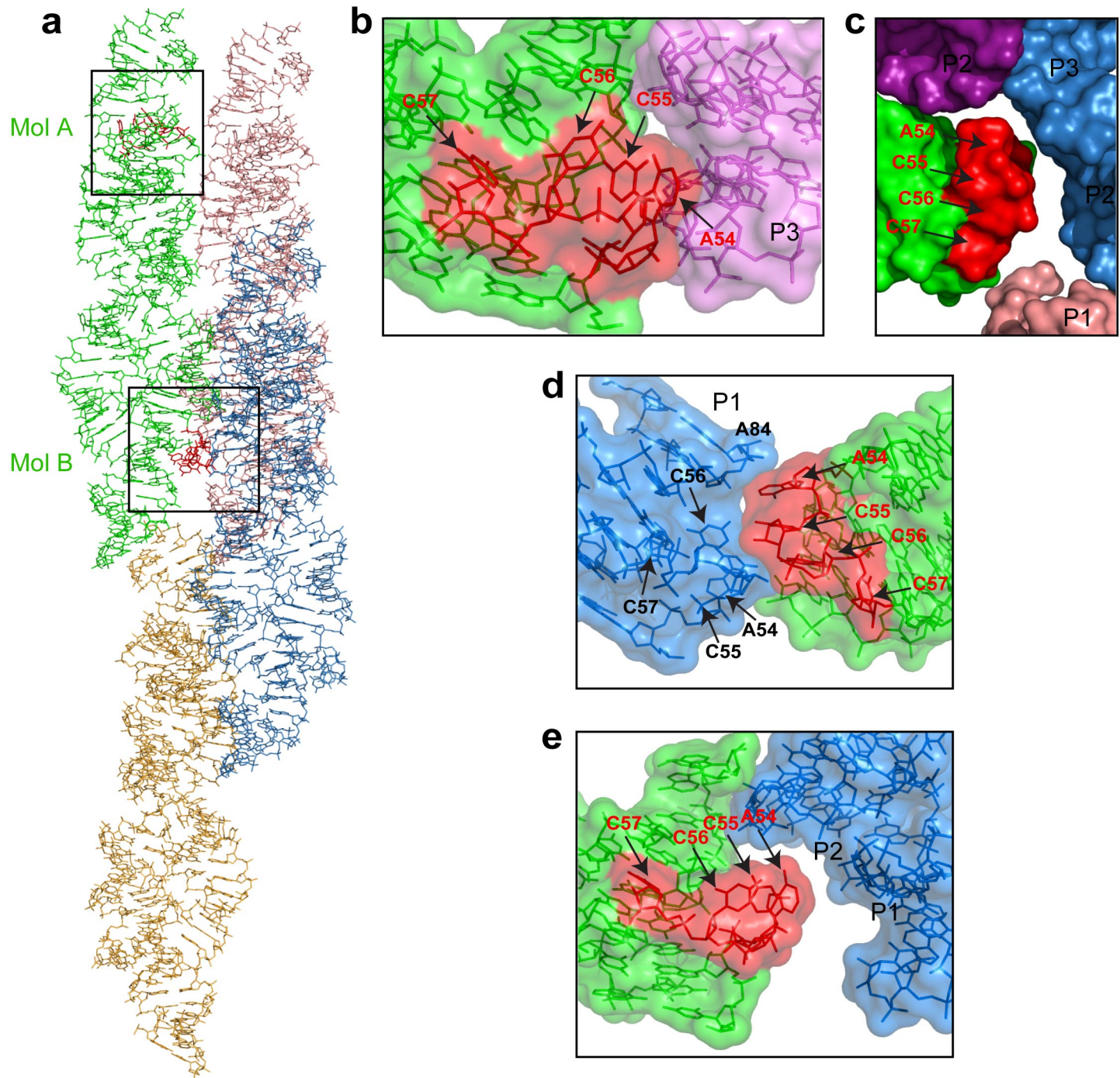
Supplementary Figure 6. Top view of the tertiary loop-loop interface in the dG and guanine riboswitches. Dashed lines depict putative hydrogen bonds. **a**, Kissing loops in the dG riboswitch (current study, PDB code 3SKI) form two G-C base pairs and several hydrogen bonds between the bases and the sugar-phosphate backbone. Residue A71 (in pink), the ‘key’, is inserted into the L2 loop. Tertiary base pairing is shown in insets on the right. **b**, In the guanine riboswitch¹⁵ (PDB code 1Y27), kissing loops form a dense network of interactions which involve five base pairs, three base-backbone hydrogen bonds and intercalation of A35 between residues of the L3 loop. Insets on the right show the formation of two tertiary base quartets that include canonical G-C base pairs also observed in the dG riboswitch. Residue A66 (in pink), analogous to A71, is not inserted into the L2 loop and instead participates in the formation of the bottom (G38-C60)•A66•A33 quartet.



Supplementary Figure 7. Electron density maps of the dG riboswitch in the nucleoside bound forms. All maps are shown with refined models of RNA and ligands. Red spheres depict water molecules. **a**, 2.3 Å refined $2F_o-F_c$ map (contoured at 1 σ level) of the A54-to-C58 fragment (molecule A) in the dG bound riboswitch (PDB ID 3SKI). **b**, Same map, molecule B. Note the slightly lower quality of the density map for the dG sugar, C56 backbone and C57 base. **c**, 2.3 Å F_o-F_c omit map (2 σ level) for bound dG in molecule A that was calculated using the structure refined without dG. Refinement of dG resulted in the C2' *endo* conformation of the sugar typical for deoxyribonucleosides. **d**, 2.6 Å refined $2F_o-F_c$ map (contoured at 1 σ level) of the A54-to-C58 fragment (molecule A) in the guanosine bound dG riboswitch (PDB ID 3SKZ). C56 is looped out and its base does not have a strong electron density map. **e**, Same map, molecule B. A54, C55 and C56 nucleotides have significantly reduced density, especially for their bases. Note that views in panels d and e are slightly tilted in comparison with panels a and b. **f**, 2.6 Å F_o-F_c omit map (2 σ level) for bound guanosine in molecule A that was calculated using the structure refined without guanosine. The refined guanosine had a C3' *endo* sugar conformation characteristic of ribonucleosides. The C3' *endo* sugar pucker appears to be predominantly defined by the electron density, not the stereochemical parameters of the ligand used during refinement, since dG molecules with the C2' *endo* sugar pucker placed in the structure instead of guanosines after refinement also adopted C3' *endo* deoxyribose conformations.



Supplementary Figure 8. Recognition of nucleotides by the dG riboswitch and electron density maps of the dG riboswitch bound to dGMP and GMP. All maps are shown with models of RNA and ligands. Red spheres depict water molecules. **a**, Recognition of dGMP by the dG riboswitch. Conformational differences (depicted by arrows) in RNA revealed by superposition of the ligand binding pockets from molecules A in the dGMP (colored) and dG (grey) bound riboswitch structures. **b**, 2.7 Å refined $2F_o-F_c$ map (contoured at 1 σ level) of the A54-to-C58 fragment (molecule A) in the dGMP bound riboswitch (PDB ID 3SLM). **c**, Same map, molecule B. A54, C55 and C56 are missing some electron density. **d**, 2.5 Å refined $2F_o-F_c$ map (1 σ level) of the A54-to-C58 fragment (molecule A) in the GMP-bound dG riboswitch (PDB ID 3SLQ). C56 is looped out and its base does not have strong electron density. **e**, Same map, molecule B. A54, C55 and C56 nucleotides are mostly disordered and only have electron density map around their phosphates.



Supplementary Figure 9. Intermolecular interactions in the vicinity of the J2-3 region in the crystals of the dG riboswitch. **a**, Packing of the riboswitch dimers (each dimer in its own color) in the $P2_12_12_1$ space group crystal of the dG riboswitch bound to dG. Similar packing arrangements are also observed in the crystals of the guanosine and GMP bound riboswitches. The A54-to-C57 regions of the J2-3 loop from the green dimer are shown in red. **b**, A zoomed-in semi-transparent surface view of the J2-3 region from molecule A of the dG bound riboswitch. The view shows that A54 is positioned within a hydrogen bond distance from a neighboring riboswitch, while other nucleotides of the J2-3 loop are not located close to other riboswitch molecules in the crystal lattice. The intermolecular space is sufficient to accommodate looped out nucleotides in the guanosine and GMP bound riboswitches. **c**, Same region in molecule B. None of the J2-3 loop nucleotides are close to the neighboring riboswitches. A54 is positioned 4.4 Å away from the P2 nucleotides of the purple molecule. **d**, The J2-3 loop in molecule A in the dGMP bound riboswitch makes contacts with the J2-3 region from another riboswitch. Note that the dGMP bound riboswitch was crystallized in the $C2$ space group with crystal packing interactions that differ from other complexes. **e**, Same region in molecule B. All nucleotides in the J2-3 regions are positioned far from the neighboring riboswitch molecules.

Supplementary Table 1. Statistics for structure determination and cation identification.

Crystal	Soaked, 2 mM [Ir(NH ₃) ₆]Cl ₃	Native	Soaked, 10 mM [Co(NH ₃) ₆]Cl ₃	Soaked, 10 mM MnCl ₂	Soaked, 10 mM CsCl
Data collection					
Space group	<i>C2</i>	<i>P2₁2₁2₁</i>	<i>C2</i>	<i>C2</i>	<i>C2</i>
Cell dimensions					
<i>a, b, c</i> (Å)	98.0, 35.0, 111.1	34.9, 47.8, 228.3	98.5, 35.0, 110.8	97.0, 34.6, 111.6	102.4, 35.4, 119.3
α, β, γ (°)	90.0, 92.5, 90.0	90.0, 90.0, 90.0	90.0, 92.2, 90.0	90.0, 92.8, 90.0	90.0, 95.2, 90.0
Wavelength (Å)	1.1052	1.0809	1.4500	1.5000	1.4000
Resolution ^a	20.00-2.90 (3.00-2.90)	20.00-2.30 (2.35-2.30)	20.00-3.10 (3.21-3.10)	20.00-3.10 (3.21-3.10)	20.00-2.95 (3.06-2.95)
R _{merge} (%) ^a	10.2 (18.0)	7.9 (27.8)	16.0 (49.7)	13.6 (24.0)	10.8 (33.5)
$\langle I \rangle / \sigma(I)$ ^a	31.2 (9.8)	16.0 (5.3)	11.2 (3.9)	19.9 (6.6)	19.6 (4.7)
Completeness (%) ^a	98.8 (92.3)	93.1 (89.4)	96.8 (98.2)	97.9 (85.2)	95.7 (98.4)
Unique reflections ^a	8,487 (764)	16,645 (1,049)	7,041 (701)	6,921 (586)	8,847 (882)
Redundancy ^a	6.5 (5.6)	6.4 (5.3)	4.2 (4.0)	5.9 (4.5)	3.3 (3.3)
Refinement (F>0)					
Resolution (Å)	20.00-2.90	20.00-2.30	20.00-3.10	20.00-3.10	20.00-2.95
Number of reflections					
Working set	7,773	13,233	5,546	6,215	14,049
Test set	405	1,678	663	317	1,556
R _{factor} / R _{free} (%)	21.9/26.4	25.3/28.1	23.6/29.9	19.6/25.2	21.7/28.7
Number of atoms					
RNA	2,826	2,903	2,810	2,826	2,826
dG	38	38	38	38	38
Cations	76	4	67	19	8
Water	5	111	18	10	2
Average B-factors(Å ²)					
RNA	48.8	38.8	49.0	64.6	93.2
dG	38.6	31.9	24.3	37.31	66.2
Cations	117.2	42.7	69.2	60.1	112.8
Water	16.2	28.7	14.3	40.1	38.2
Rmsd					
Bond lengths (Å)	0.006	0.006	0.006	0.006	0.006
Bond angles (°)	1.008	0.983	1.145	1.132	1.045
Coordinate error ^b	0.45	0.21	0.63	0.47	0.41

^a Values for the highest-resolution shell are in parentheses.

^b Estimated coordinate error based on maximum likelihood was calculated with REFMAC⁵⁰ or PHENIX⁴⁹.

Supplementary Table 2. Crystallographic statistics for riboswitches with bound dG analogs.

Crystal	Guanosine	dGMP	GMP
Data collection			
Space group	<i>P2₁2₁2₁</i>	<i>C2</i>	<i>P2₁2₁2₁</i>
Cell dimensions			
<i>a, b, c</i> (Å)	34.8, 47.2, 228.3	96.0, 66.1, 72.5	34.9, 48.4, 228.6
α, β, γ (°)	90.0, 90.0, 90.0	90.0, 118.0, 90.0	90.0, 90.0, 90.0
Wavelength (Å)	1.0750	1.0750	1.0750
Resolution ^a	20.00-2.60 (2.69-2.60)	20.00-2.70 (2.80-2.70)	20.00-2.50 (2.59-2.50)
R _{merge} (%) ^a	6.6 (20.9)	9.6 (59.9)	7.6 (37.6)
$\langle I \rangle / \sigma(I)$ ^a	39.0 (7.8)	19.3 (2.6)	27.6 (5.0)
Completeness (%) ^a	90.3 (87.2)	100 (100)	96.5 (98.8)
Unique reflections ^a	11,024 (1,046)	11,084 (1,100)	13,677 (1,343)
Redundancy ^a	8.4 (8.9)	4.0 (4.1)	4.6 (4.8)
Refinement (F>0)			
Resolution (Å)	20.00-2.60	20.00-2.70	20.00-2.50
Number of reflections			
Working set	10,390	9,930	12,209
Test set	520	1,082	1,362
R _{factor} / R _{free} (%) ^a	21.9/27.5	20.0/24.5	23.7/28.5
Number of atoms			
RNA	2,908	2,908	2,874
Ligands	40	46	48
Cations	3	3	0
Water	7	10	2
Average B-factors(Å ²)			
RNA	58.7	37.7	50.9
Ligands	53.9	33.6	52.2
Cations	58.5	39.3	-
Water	33.2	27.4	29.8
Rmsd			
Bond lengths (Å)	0.006	0.006	0.006
Bond angles (°)	1.000	0.992	1.058
Coordinate error ^b	0.46	0.77	0.46
^a Values for the highest-resolution shell are in parentheses.			
^b Estimated coordinate error based on maximum likelihood was calculated with REFMAC ⁵⁰ or PHENIX ⁴⁹ .			